

AD-A160 656

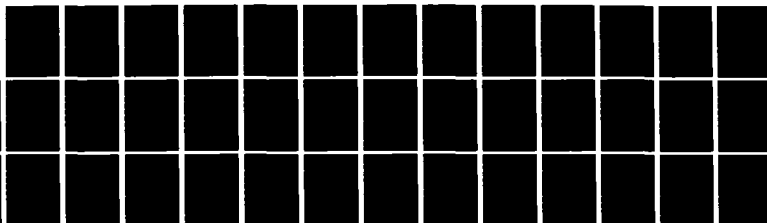
SAXS (SMALL ANGLE X-RAY SCATTERING) STUDY OF MICELLE
FORMATION IN MIXTURE. (U) CINCINNATI UNIV OH DEPT OF
MATERIALS SCIENCE AND ENGINEERING. D RIGBY ET AL.
01 NOV 85 TR-2 N00014-85-K-0245

1/1

UNCLASSIFIED

F/G 7/4

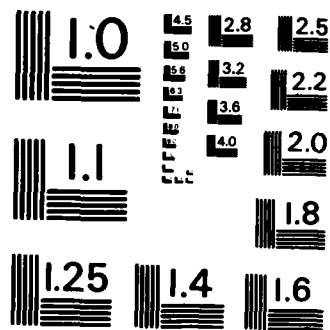
NL



END

FILMED

DTIC



MICROCOPY RESOLUTION TEST CHART
NATIONAL BUREAU OF STANDARDS - 1963 - A

9

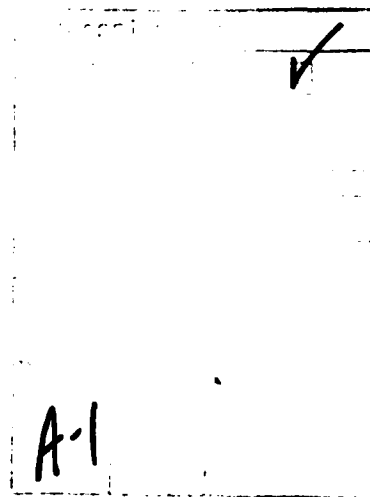
AD-A160 656

SECURITY CLASSIFICATION OF THIS PAGE (When Data Entered)

REPORT DOCUMENTATION PAGE		READ INSTRUCTIONS BEFORE COMPLETING FORM
1. REPORT NUMBER No. 2	2. GOVT ACCESSION NO. AD-A160 656	3. RECIPIENT'S CATALOG NUMBER
4. TITLE (and Subtitle) SAXS Study of Micelle Formation in Mixtures of Butadiene Homopolymer and Styrene-Butadiene Block Copolymer. 2. Effects of Block Lengths		5. TYPE OF REPORT & PERIOD COVERED Technical Report
		6. PERFORMING ORG. REPORT NUMBER
7. AUTHOR(s) D. Rigby and R. J. Roe		8. CONTRACT OR GRANT NUMBER(s) N00014-85-K-0245
9. PERFORMING ORGANIZATION NAME AND ADDRESS University of Cincinnati Cincinnati, OH 45221		10. PROGRAM ELEMENT, PROJECT, TASK AREA & WORK UNIT NUMBERS NR 356-655
11. CONTROLLING OFFICE NAME AND ADDRESS Office of Naval Research 800 North Quincy Street Arlington, VA 22217		12. REPORT DATE November 1, 1985
14. MONITORING AGENCY NAME & ADDRESS (if different from Controlling Office)		13. NUMBER OF PAGES 38
		15. SECURITY CLASS. (of this report) Unclassified
		15a. DECLASSIFICATION/DOWNGRADING SCHEDULE
16. DISTRIBUTION STATEMENT (of this Report) Approved for public release; distribution unlimited.		
17. DISTRIBUTION STATEMENT (of the abstract entered in Block 20, if different from Report) <div style="text-align: right;">DTIC ELECTE OCT 28 1985 B</div>		
18. SUPPLEMENTARY NOTES		
19. KEY WORDS (Continue on reverse side if necessary and identify by block number) Block Copolymer. Micelle. Small-angle X-ray Scattering. Polystyrene. Styrene-butadiene block copolymer.		
20. ABSTRACT (Continue on reverse side if necessary and identify by block number) The small-angle X-ray scattering technique is utilized to determine the characteristics of micelles formed in the mixtures containing a low molecular weight polybutadiene and a styrene-butadiene diblock copolymer. Three different block copolymers of about the same overall molecular weight but with differing lengths of the two blocks are utilized. The observed scattering curve is fitted with a calculated one based on a model of		

DTIC FILE COPY

polydisperse micelles interacting with each other according to the Percus-Yevick hard-sphere fluid approximation. The following quantities characterizing the structure of the micelle are evaluated as a function of temperature and copolymer concentration: the average radius of the core, the polydispersity of the core radius, the apparent hard-sphere radius of interaction, the critical micelle concentration, the degree of swelling of the core, and the number density of the micelles. The critical micelle concentration decreases as the proportion of styrene in the copolymer increases. The size of the micelles of a given copolymer remains independent of concentration but shows a moderate variation with temperature, especially immediately before the final dissolution temperature. The degree of swelling of the core by polybutadiene increases steadily with increasing temperature.



OFFICE OF NAVAL RESEARCH

Contract N00014-85-K-0245

Task No. NR 356-655

TECHNICAL REPORT NO. 2

SAXS Study of Micelle Formation in Mixtures of
Butadiene Homopolymer and Styrene-Butadiene Block Copolymers.
2. Effects of Block Lengths

by

D. Rigby and R. J. Roe

Accepted for Publication

in

Macromolecules

Department of Materials Science
and Engineering
University of Cincinnati
Cincinnati, Ohio 45221-0012

November 1, 1985

Reproduction in whole or in part is permitted for
any purpose of the United States Government.

This document has been approved for public release
and sale; its distribution is unlimited.

85 10 28 053

INTRODUCTION

Block copolymers present a variety of morphology arising from microphase separation of constituent blocks into spheres, cylinders, or lamellae. With a change in temperature such an ordered structure can be transformed into disordered, homogeneous phase.^{1,2} When a diblock copolymer AB is mixed with a homopolymer A, the mixture may either exist as an (ordered or disordered) single phase or undergo a macrophase separation. The temperature of order-disorder transition of the microdomain structure is also affected^{3,4} by the addition of the homopolymer. Thus, the phase diagrams⁴ of mixtures containing a diblock copolymer and a homopolymer exhibit a fascinating complexity involving macroscopic and microscopic phase separations.

In the present study we are interested in one part of the overall phase diagram, namely that involving small amounts of copolymer mixed with much larger amounts of homopolymer. This region of the phase diagram was investigated in least detail in our previous study.⁴ Typical features of behavior found in this work may be summarized as follows. When the block copolymer content is very low, all the copolymer molecules are molecularly dissolved in the homopolymer, resulting in a single phase mixture. With increase in the copolymer content, eventually a point is reached (the critical micelle concentration) at which the homopolymer is unable to solubilize any additional

copolymer molecules. Beyond the CMC the excess copolymers segregate to form microdomains, or micelles, dispersed in the homopolymer-rich matrix. These micelles, presumably of spherical shape, consist of the central core comprising predominantly of copolymer B blocks, and the surrounding shell, or corona, within which copolymer A blocks and homopolymer A molecules are intermixed. In the dilute suspension of such micelles, aggregation (or flocculation) of the micelles themselves is discouraged, owing to unfavorable entropic factors⁵ which come into play when the coronae of neighboring micelles overlap. Further increase in the amount of added copolymer may eventually lead to the onset of macroscopic phase separation, giving rise to two coexisting phases, one of them (the "solid-like" phase) containing ordered arrays of densely packed micelles and the other (the "liquid-like" phase) consisting of a dilute suspension of independent micelles.

In a recent publication⁶ (Part I of the present series) we have shown that small-angle X-ray scattering technique can be utilized to determine the characteristics of block copolymer micelles suspended in a homopolymer matrix. Applying the technique to the mixtures containing a low molecular weight polybutadiene and a styrene-butadiene diblock copolymer consisting of approximately 50% styrene, we evaluated the following parameters characterizing the

micelles as a function of temperature and copolymer concentration: the critical micelle concentration, the radius of gyration of the core, the degree of swelling of the core, the number of copolymer molecules per micelle, and the number of micelles per unit volume of the mixture. In the present work we apply the technique to two further series of mixtures containing the same polybutadiene and one of two other styrene-butadiene diblock copolymers (consisting of 25% and 75% styrene, respectively). The three diblock copolymers have about the same molecular weight, and the results thus reveal the effect of block lengths on the micelle characteristics. Recently, theories of block copolymer micelle formation were developed by two groups^{7,8} of workers, and in a separate paper⁹ we make a detailed comparison of the results obtained here with the prediction of the theory by Leibler et al.⁷

EXPERIMENTAL SECTION

Characterization data for the polymers used are summarized in Table 1. The butadiene homopolymer is sample CDS-B-3 obtained from Goodyear Chemical Company, who also provided its characterization data. The three styrene-butadiene block copolymers were kindly synthesized for us by Dr. H. L. Hsieh of Philips Petroleum Company, who supplied the molecular weight and M_w/M_n data. The styrene contents were investigated in this laboratory using a

Varian T60A NMR spectrometer. In general, the results of our analysis agree well with those of Krause et al.¹⁰ who have performed an independent characterization of the same samples.

As the styrene content of the copolymers is decreased, the solubility of copolymer in the homopolymer is increased. Thus at room temperature it was found that the CMC was 7.8%, 0.26%, and 0.10% for the mixtures containing samples 25/75, 50/50, and 75/25, respectively. Accordingly, the composition ranges of interest in the present work are different for the three copolymers studied, and the copolymer concentration ranges varied between 7.5% and 22% for sample 25/75, between 0.5% and 8% for sample 50/50, and between 0.5% and 3% for sample 75/25.

All samples were prepared by mechanical mixing under vacuum at temperatures between 200°C and 220°C. This use of elevated temperatures was to ensure that the mixture was in a region of the phase diagram corresponding to a single homogeneous phase in order that intimate mixing of copolymer and homopolymer was achieved before the formation of micelles on subsequent cooling.

All the scattering data obtained at various temperatures thereafter were independent of the thermal history of the sample as long as the opportunity for thermal degradation by exposure to high temperature was avoided. Some of the measurements were performed over a time period

varying from 20 minutes to 14 hours after attainment of a constant temperature, and yet no observable change could be noticed with elapse of time. We believe the phenomena reported here correspond essentially to equilibrium conditions.

All scattering curves were obtained using a Kratky camera coupled with a Tennelec one-dimensional position sensitive detector and its associated electronics.¹¹ Nickel-filtered $\text{CuK}\alpha$ radiation supplied by a Philips XRG 3100 generator operating at 45kV and 35mA was used throughout. After transferring to a PDP 11/23 laboratory computer, the data was subjected to various manipulations, including applying corrections for non-uniformity of the detector sensitivity along its length and for absorption of the primary beam by the sample. This was followed by scaling to absolute units using a Kratky Lupolen standard, and correction for slit-length collimation error using Strobl's algorithm.¹²

In all cases a background corresponding to that obtained from polybutadiene homopolymer at the same temperature was subtracted from the scattering curves. The effect of using only the pure polybutadiene scattering as background is to neglect possible contributions from copolymer molecules dissolved in the homopolymer-rich phase. This is certainly justifiable when the CMC is low, although it is not obvious that it should remain so when the CMC is

of the order of several percent. To assess the effects of neglecting this additional contribution, we compared scattering curves of mixtures containing sample 25/75 at 30°C that were obtained by subtracting only a polybutadiene background with those obtained after subtracting the measured scattering of a mixture at the CMC (in this case 7.8%). The micelle radii deduced by these two methods showed very good agreement, and therefore the simpler approach of subtracting a pure polybutadiene background was adopted for all mixtures.

ANALYSIS OF DATA

The z-average radius of gyration R_g of the micelle core was determined in Part I by analyzing the scattered intensity $I(s)$ according to the Guinier law

$$I(s) = I(0) \exp (-4\pi^2 R_g^2 s^2 / 3) \quad (1)$$

where s is equal to $2 \sin \theta / \lambda$. The Guinier law is valid for a very dilute suspension of independent particles. When, at any finite concentration, the particles interact with each other and their positions in space are no longer random, the effect of interference of X-rays scattered by individual particles leads to deviation from equation (1). More generally, the intensity scattered from unit volume of an isotropic material containing N identical particles can be written as

$$I(s) = N |F(s)|^2 S(s) \quad (2)$$

where $F(s)$ is the single particle form factor and $S(s)$ denotes

the interference function defined by

$$S(s) = (1/N) \sum_n \sum_n' \exp (2\pi i s r_{nn'}) \quad (3)$$

For a dilute system, where the positions of the particles are random in space, $S(s)$ is equal to unity for all s and hence the scattered intensity reduces to $N|F(s)|^2$, which can then be approximated by the Guinier equation (1) for small s . At finite concentrations $S(s)$ falls below unity for small s , and the possible methods for correcting for this interparticle interference effect were discussed by a number of workers.¹³⁻¹⁵ For our system, the most satisfactory approach appears to be one based on the Percus-Yevick solution of hard-sphere fluids.

The Percus-Yevick integral equation¹⁶ provides an excellent approximation for calculating thermodynamic functions of fluids of interacting particles. Moreover, the solution of Percus-Yevick equation for hard-sphere fluids can be obtained in closed form. The scattering function calculated from the Percus-Yevick approximation was already utilized to analyze scattering data from microemulsions¹⁷ and from bulk block copolymers¹⁸ having ordered microdomain structure. Recently, Leibler and Pincus⁵ estimated the potential energy of interaction of two block copolymer micelles from the consideration of the overlap of segments belonging to the coronae as they approach each other. The calculated potential energy curve as a function of the inter-micellar distance is very steep, and can justifiably be approximated by a hard-sphere potential.

For a spherical particle of radius R the form factor is given by

$$F(s) = (\Delta\rho/2\pi^2s^3) [\sin(2\pi sR) - 2\pi sR \cos(2\pi sR)] \quad (4)$$

where $\Delta\rho$ is the difference in electron density between the particle and the surrounding medium. $|F(s)|^2$ given by equation (4) exhibits steep minima at regular intervals of s beyond the Guinier region. No corresponding minima were observed in our X-ray data and we attribute this to the non-uniformity of the core radii. The scattering function for fluids of polydisperse hard spheres was recently calculated in the Percus-Yevick approximation by Vrij and coworkers^{19,20} and by Blum and Stell.²¹ A similar, but more approximate, expression was also derived by Kotlarchyk and Chen²² on the assumption that the position of the particles in the fluids are uncorrelated to the particle size. With our system the single particle form factor is related to the radius R of the micelle core, while the interparticle interference is governed by the effective hard-sphere radius R_{HS} which is approximately equal to the overall radius of the micelle including the corona. The size distributions of R_{HS} and R are not well correlated to each other since the thickness of the corona depends on the length distribution of the copolymer A blocks but the core radius does not. With our system, therefore, it would be more appropriate to use the Kotlarchyk-Chen approximation²² rather than the more exact results of Vrij and Blum. Moreover, the Kotlarchyk-Chen approximation requires much less computation, and yields

scattering curves which are practically indistinguishable from the exact results except at very small angles which are below the range of our measurements.

For a polydisperse collection of particles equation (2) is replaced by

$$I(s) = N \langle |F(s)|^2 \rangle S'(s) \quad (5)$$

where $S'(s)$ is now the "apparent" interference function. When the particle size and the position are uncorrelated, $S'(s)$ can be written as

$$S'(s) = 1 + \beta(s) [S_{av}(s) - 1] \quad (6)$$

where

$$\beta(s) = \langle |F(s)|^2 \rangle / \langle |F(s)|^2 \rangle \quad (7)$$

and $S_{av}(s)$ is the monodisperse interference function for particles of some average radius.

To evaluate the averages of the form factor $F(s)$ indicated by equations (5) and (7), we assume the micelle core radii to be distributed according to the Flory-Schulz distribution

$$W(R) = (1/Z!) b^{Z+1} R^Z \exp(-bR) \quad (8)$$

The parameter Z characterizes the width of the distribution, with a value of $Z = \infty$ corresponding to a delta function. The parameter b is related to the reciprocal mean radius, i.e., $b = (Z+1)/\langle R \rangle$. The moments of R about the origin are given by

$$\langle R^p \rangle = (Z+p)! / (Z! b^p) \quad (9)$$

The Flory-Schulz distribution is chosen here for its convenience, since it allows analytical evaluation of the integrals required for $\langle |F(s)|^2 \rangle$ and $\langle |F(s)|^2 \rangle$ when $F(s)$ is given by equation (4). The resulting explicit expressions can be found in the literature.^{22,23}

For the monodisperse interference function $S_{av}(s)$ we utilize the closed-form solution to the Percus-Yevick approximation for hard-sphere fluids given by Ashcroft and Lekner,²⁴

$$S_{av}(s) = [1 + 24\xi G(A, \xi)/A]^{-1} \quad (10)$$

where ξ is the hard-sphere volume fraction equal to $N(4\pi/3)\langle R_{HS} \rangle^3$, $\langle R_{HS} \rangle$ being the average hard-sphere radius, and A is equal to $4\pi s \langle R_{HS} \rangle$. $G(A, \xi)$ is a function of A and ξ , and its explicit expression can be found in the original paper²⁴ (see also Kinning and Thomas¹⁸).

Our theoretical model for the calculation of intensity $I(s)$ then consists of equation (5) in conjunction with equations (4), (6)-(8), and (10). The calculated intensity was fitted to the experimental data by adjusting the four parameters -- Z , $\langle R \rangle$, $\langle R_{HS} \rangle$ and the scaling constant (the latter being related to the product $N(\Delta \rho)^2$) -- to determine their best values. Numerically this was accomplished by minimizing the deviation

$$\epsilon^2 = \sum_s [1/\sigma^2(s)] [I_{obs}(s) - I_{calc}(s)]^2 \quad (11)$$

where $I_{obs}(s)$ is the slit-desmeared intensity and $\sigma(s)$ is the error associated with $I_{obs}(s)$ as a result of the counting statistics and its propagation through the slit-desmearing computation.¹²

The following two examples illustrate the steps we adopted for achieving this four-parameter minimization procedure. The data in Figure 1 were obtained with a mixture containing 8% sample 50/50 and Figure 2 with a mixture containing 3% sample 75/25, both at 30°C. The solid curves are the best fitting curves obtained by the four-parameter minimization procedure (the best values of the parameters obtained are: $Z = 55$, $\langle R \rangle = 8.96\text{nm}$, $\langle R_{\text{HS}} \rangle = 15.7$, and $N(\Delta\rho)^2 = 0.0323 \text{ electron}^2/\text{nm}^3$ for Figure 1, and $Z = 6$, $\langle R \rangle = 8.41$, $\langle R_{\text{HS}} \rangle = 11.8$, and $N(\Delta\rho)^2 = 0.0108$ for Figure 2). The broken curves were obtained with the assumption of monodisperse core diameters, that is, by forcing $Z = \infty$ (the best values of the parameters obtained are $\langle R \rangle = 9.4\text{nm}$, $\langle R_{\text{HS}} \rangle = 16.5$, and $N(\Delta\rho)^2 = 0.0301 \text{ electron}^2/\text{nm}^9$ for Figure 1, and $\langle R \rangle = 13.4$, $\langle R_{\text{HS}} \rangle = 18.8$, and $N(\Delta\rho)^2 = 0.0054$ for Figure 2). In the case of Figure 1, where the concentration of copolymer is moderately high, the interparticle interference causes the peak to appear at $s = \sim 0.027\text{nm}^{-1}$, and $\langle R_{\text{HS}} \rangle$ is essentially determined by the position of the peak irrespective of the assumption of polydispersity or monodispersity. In the case of Figure 2, where the concentration of copolymer is low, the interparticle interference effect is very small, and the choice of the value of $\langle R_{\text{HS}} \rangle$ is dictated primarily by the scattering curve at small angles, and does not substantially affect the shape of the curves at higher angles. Subsequently, therefore, we evaluated $\langle R_{\text{HS}} \rangle$ first under the monodisperse assumption, and the same fixed value of $\langle R_{\text{HS}} \rangle$ was then utilized to seek the best values of the other parameters.

The monodisperse curves totally fail to fit the observed data at high s . The fit is greatly improved by introducing the polydispersity but still some discrepancies remain. (Note that the ordinate in Figures 1 and 2 is in logarithmic scale, so that the discrepancy at high s is exaggerated.) The best values of Z obtained indicate that the polydispersity is fairly large, especially in the case of the data shown in Figure 2. In the model we have not included the possibility of the boundary between the core and the corona being diffuse. Our previous analysis^{1,3} of the small-angle X-ray data obtained with bulk or concentrated block copolymer samples showed the interface to be relatively sharp (between 5 to 9 Å). The effect of including the diffuse interface into the model is to multiply^{1,18,25,26} the single particle form factor (4) by $\exp(-4\pi^2\sigma^2s^2)$ where σ is proportional to the thickness of the interface. The intensity calculated by equation (5) would then decrease more rapidly with increasing s when the interface is more diffuse. If we had assumed the interface thickness to be about 20 Å, as suggested by some other workers,²⁷⁻³³ we would have required much smaller values of Z (implying unreasonably large polydispersity) in order to be able to fit the observed curves at high angles.

Finally we give a brief remark about how the radius of gyration obtained by the present curve fitting method compares with the value obtainable from the Guinier analysis by use of equation (1). When the two methods were applied to the data obtained with the mixture containing 4% of sample 50/50, the z -average radius of gyration obtained by the Guinier analysis

(and reported in Part I) was larger by at most 2% than the value determined by the present curve fitting method. Similar good agreements were realized with all the data obtained with samples 25/75 and 50/50 (both of which gave fairly large Z values, namely fairly narrow polydispersity, on curve fitting). Such good agreements arise partly from a fortunate cancellation of errors. With moderate concentration of particles, the interference function $S(s)$ or $S'(s)$ deviates appreciably from unity only at very small angles (smaller than the reciprocal of the average interparticle distance). In utilizing the data obtained only between 0.02 and 0.05nm^{-1} in s , as we have done, the distortion of the Guinier law by the interparticle interference was largely avoided. As s increases the Guinier law progressively fails to represent the single particle form factor adequately, and this leads to the consequence that the Guinier analysis tends to overestimate the radius of gyration of monodisperse particles. The polydispersity of the particles, on the other hand, tends to make the Guinier estimate fall below the true radius of gyration, and the errors from these two sources largely cancel each other. In the case of mixtures containing sample 75/25, however, the polydispersity found from the curve fitting was very large, and consequently the radii of gyration obtained from the straight Guinier analysis were smaller by as much as 20% than the values determined by the curve fitting procedure.

RESULTS AND DISCUSSION

Variation of the z-average radius $\langle R \rangle_z$ of the micelle core ($\langle R \rangle_z^2 = \langle R^8 \rangle / \langle R^6 \rangle$) with temperature is shown in Figure 3 for mixtures containing 14% sample 25/75, 4% sample 50/50, and 3% sample 75/25. The general features of the observed behavior are best described with reference to the curve obtained with sample 75/25, in which we observe that the size remains fairly constant up to ca. 90°C. Above this temperature $\langle R \rangle_z$ decreases slightly before passing through a minimum and then increasing again about 20-40° below the temperature at which the micelles finally dissolve. (In the example shown, the micelles dissolve around 192°C, but the data at temperatures above 160°C are too imprecise to permit application of the curve fitting procedure.) The curves obtained with samples 25/75 and 50/50 appear to show the same trends but are shifted to lower temperatures in accordance with the increased degree of compatibility between the copolymer and homopolymer. As a result, sample 50/50 shows only the portion of the curve in which $\langle R \rangle_z$ decreases, passes through a minimum and then increases again, whilst sample 25/75 shows only the latter increasing portion in the temperature range studied. In addition, the increases in $\langle R \rangle_z$ before dissolution appear more pronounced as we move from sample 75/25 through 50/50 to 25/75. For the same copolymer the variation in $\langle R \rangle_z$ with concentration is very minor (probably within the experimental error), except that the increase in $\langle R \rangle_z$ before dissolution occurs over a different temperature range since the dissolution temperature depends on concentration. This increase in $\langle R \rangle_z$ at higher

temperatures was found to occur for all mixtures studied with the exception of those containing 6% and 8% of sample 50/50. These two mixtures set themselves apart from all others in that they are the only two which give a low-angle interparticle interference maximum in the scattering curves as illustrated in Figure 1. Hence the tendency for $\langle R \rangle_z$ to increase with temperature before dissolution appears to be a characteristic of micellar suspensions with no strong correlation between micelles.

Recently, Selb et al.³⁴ utilized the neutron scattering technique to determine the core radius of micelles of styrene-butadiene diblock copolymers suspended in polybutadiene matrix. They determined $\langle R \rangle$ from the position of a subsidiary maximum observed in their scattering intensity curve. One of their block copolymers, having the styrene content of 48% and the overall molecular weight of 29000, is comparable to our sample 50/50. The core radius of the micelles formed by this copolymer was determined to be 9.6 and 11.5nm when 2% of the copolymer was mixed at room temperature with polybutadienes of molecular weights 1600 and 3300, respectively. Their values therefore agree fairly well with our value $\langle R \rangle_z = 10.2\text{nm}$ (see in Figure 3) obtained at room temperature with the mixture containing 4% sample 50/50 in polybutadiene of molecular weight 2350.

The ratio $\langle R_{HS} \rangle / \langle R \rangle$ was found to be approximately constant for mixtures containing the same copolymer, and was equal to ca. 2.0, 1.7, and 1.4 for samples 25/75, 50/50, and 75/25, respectively. These ratios follow a trend as expected from the relative lengths of the two blocks in the copolymer. If both the

radius of the core and the thickness of the corona were comparable to the average end-to-end distances of the B and A blocks, respectively, the ratios would have been equal to 2.9-3.6, 2.1-2.5, and 1.7-1.9 for the three copolymers. (The ranges reflect the uncertainties in the literature values³⁵ of the ratio of end-to-end distance to molecular weight for polystyrene and polybutadiene.) The observed ratios are smaller than these idealized values, and we can think of at least two reasons for this. (1) The radii of the core given in Figure 3 are larger than the end-to-end distance of the styrene blocks, especially in the case of samples 25/75 and 50/50 which have relatively short styrene blocks. For example, the observed $\langle R \rangle$ for sample 25/75 at 50°C is equal to ca. 11nm, which is between the estimated rms end-to-end distance 5.5nm and the fully extended length 17.7nm. (2) The chains in the corona are much less likely to be stretched and therefore the thickness of the corona is probably much more comparable to the rms end-to-end distance, although no direct measure of the corona thickness is now available. The hard sphere radius $\langle R_{HS} \rangle$ deduced from the interparticle interference effect should, however, be smaller than the overall radius of the micelle including the corona, since the strong repulsion between micelles probably develops only after some degree of overlap between two coronae has been realized.

In the curve fitting procedure to evaluate the best values of the parameters, the polydispersity parameter Z can only be determined with least certainty, because the value of Z is mostly

governed by the shape of the scattering curve at relatively high s where the intensity $I(s)$ is low and the error $\sigma(s)$ high (see Figures 1 and 2). The value of Z is affected also by the features of the model itself, for example whether we allow the possibility of the core-corona interface being diffuse. For this reason it is difficult to discuss any consistent trend in the value of Z with the variation in temperature or concentration. Among the three copolymers, however, it appears that the polydispersity for sample 75/25 is always larger than that for sample 50/50 or sample 25/75. We may express the polydispersity by the more familiar ratio, V_w/V_n , which is related to Z by

$$\begin{aligned} V_w/V_n &= \langle R^6 \rangle / \langle R^3 \rangle^2 \\ &= (Z+6)(Z+5)(Z+4) / (Z+3)(Z+2)(Z+1) \end{aligned} \quad (12)$$

The ratio V_w/V_n is equal to 2.8 ± 1.2 , 1.4 ± 0.3 , and 1.3 ± 0.2 for samples 75/25, 50/50, and 25/75, respectively. At present we do not have any explanation as to why sample 75/25 exhibits a broader distribution of micelle sizes than other samples.

The critical micelle concentration (CMC) can be determined if we plot the intensity of micellar scattering against concentration and extrapolate the plot to zero intensity. Either the intensity $I(s)$ at a fixed s or the invariant Q , obtainable from integration of $s^2 I(s)$ over s , can serve the purpose. The determination of CMC is illustrated in Figure 4, in which the intensity $I(s)$ at $s = 0.03 \text{ nm}^{-1}$ is plotted against the concentration of sample 75/25. The points exhibit good linear relationship, and as a result the CMC can be determined to a fair

degree of precision. At higher temperatures, when there are insufficient data to construct such plots, we have used the alternative procedure of plotting the intensity against temperature at various concentrations. This is analogous to the plot, shown previously in Part I, of the zero angle intensity $I(0)$ against temperature, in which it was observed that the low angle intensity drops suddenly over a 5-10°C interval as the temperature is raised to the point at which the micelles finally dissolve.

Variation of the CMC with temperature, as determined by these two complementary methods, is illustrated in Figure 5 for the three copolymer samples studied. Here we have plotted temperature against CMC, so that the resulting curves resemble conventional binodals obtained with mixtures which undergo macroscopic phase separation. The levelling off of the curves suggests a limiting temperature above which micelle formation will not occur for a given copolymer, and which itself is somewhat sensitive to the degree of compatibility between the copolymer and homopolymer. We estimate that these upper temperatures for micelle formation lie in the ranges 60-70°C, 120-130°C, and 210-220°C for sample 25/75, 50/50 and 75/25, respectively. These trends are in qualitative agreement with our expectation, since the effective interaction energy density Λ between a copolymer and a homopolymer can be given³⁴ approximately by $(1-f_B)^2 \Lambda_{SB}$, where f_B denotes the fraction of butadiene in the copolymer and Λ_{SB} denotes the interaction energy density between styrene and butadiene homopolymers.

The volume fraction η of styrene units within the micelle core and the number N of micelles per unit volume can be determined by noting the following relations

$$N\langle |F(0)|^2 \rangle = N(\Delta\rho)^2\langle V^2 \rangle \quad (13)$$

$$\phi = N\langle V \rangle\eta + \phi_c(1-N\langle V \rangle\zeta^3) \quad (14)$$

where V denotes the micelle core volume, ϕ and ϕ_c denote the overall concentration (volume fraction) of styrene units in the mixture and the overall styrene concentration at the CMC, respectively, and ζ is the ratio R_{HS}/R . Equation (13) follows from equation (4). The first term in equation (14) represents the overall volume fraction of styrene units in the cores and the second term the overall volume fraction of styrene units in the matrix outside the micelle cores and coronae. (It assumes that the copolymer molecules dissolved in the polybutadiene matrix do not penetrate the coronae.) If the cores are swollen with polybutadiene and contain only a fraction η of styrene, then the electron density difference between the micelle cores and the homopolymer matrix is equal to $\eta\Delta\rho_{SB}$, where $\Delta\rho_{SB}$ denotes the corresponding difference between pure polystyrene and polybutadiene. In equations (13) and (14) the parameters $N\langle |F(0)|^2 \rangle$, $\langle V \rangle$, $\langle V^2 \rangle$, and ζ are obtained by the curve fitting procedure described in the previous section, ϕ_c is given by the CMC determined as described above, and ϕ is defined from the composition of the mixture. The two remaining parameters η and N can therefore be obtained by solving equations (13) and (14) simultaneously.

In calculating η and N , $\Delta\rho_{SB}$ was calculated from the following relations giving the temperature dependence of the specific volume of polystyrene and polybutadiene. For polystyrene

$$v_{PS} = 0.9217 + 5.412 \times 10^{-4}t + 1.687 \times 10^{-7}t^2 \quad (\text{above } T_g) \quad (15)$$

$$v_{PS} = 0.9369 + 2.006 \times 10^{-4}t + 2.470 \times 10^{-7}t^2 \quad (\text{below } T_g) \quad (16)$$

and for polybutadiene

$$v_{PB} = 1.1138 + 8.24 \times 10^{-4}t \quad (17)$$

where t is in degree centigrade. Equation (15) for v_{PS} above T_g and the second and third terms in equation (16) for v_{PS} below T_g were taken from Richardson and Savill.³⁷ The first term in equation (16) was calculated from equation (15) on the assumption that the T_g for the swollen polystyrene core is around 45°C, for the same reason as was discussed in Part I. Equation (17) for v_{PB} is based on the specific volume of polybutadiene at 30°C determined in this work in conjunction with the temperature coefficient obtained from the literature.³⁵

In Figure 6 the styrene volume fraction η is plotted as a function of temperature for the various mixtures indicated. For a particular copolymer the variation of η with temperature is fairly similar for all concentrations. In contrast, the behavior found for different copolymers shows interesting differences. With sample 75/25 it is seen that η values remain close to unity up to about 100°C but then show a steady, almost linear, decrease with further increase in temperature before the micelles finally

disappear. This tendency for η to decrease is also observed with the other two copolymer samples but is shifted to lower temperature. Thus there is again a suggestion that if measurements could be made at temperatures below 30°C, then samples 25/75 and 50/50 would show curves with the same overall shape as found with sample 75/25, but with η falling below unity above ca. -20°C and +25°C for samples 25/75 and 50/50, respectively.

The value of η , by definition, cannot exceed unity. Some of the η values plotted in Figure 6 are larger than one, probably reflecting the error in its evaluation. The value of η calculated is fairly insensitive to variations in the adjustable parameters evaluated by minimization of ϵ in equation (11) as long as they give a reasonably good fit to the observed curve. Sets of parameter values with $\langle R \rangle$ differing by as much as 50% were found to produce a difference in η of only 10%. After some effort in the error analysis we came to the conclusion that the major part of the error is probably in the calibration of the X-ray instrument with respect to the conversion factor required for scaling the observed intensity into absolute units. Determination of this conversion factor within 10% error is normally difficult.

The dependency on temperature of the micelle number density N is shown in Figure 7 for mixtures containing 3% sample 75/25 and 4% sample 50/50. Both curves exhibit the trend of going through a maximum on increasing the temperature before the micelles finally dissolve. We observe that the rise and fall in

N occur over the temperature range where the η value decreases steadily as seen in Figure 6 and at the same time the micelle core radius goes through a minimum as seen in Figure 3. The temperature range in which it was feasible to study sample 25/75 (up to 50°C) is such that there is insufficient data to state whether a trend of N increasing to a maximum would also be observed for this third copolymer.

Summarizing the results given above, it can be stated that, in general, the same overall trends in behavior with increasing temperature occur for all three copolymer samples studied, but the features are shifted to higher temperatures as the degree of copolymer-homopolymer compatibility decreases as a result of increased styrene block lengths. Thus, when the two polymers are highly incompatible, the copolymer aggregates in the form of micelles with cores consisting almost exclusively of copolymer styrene blocks. As the temperature is raised, the system enters an intermediate region in which the formation of micelles is still energetically favored but with some polybutadiene in addition to copolymer styrene blocks present in the cores. Finally, as the temperature is increased still further, the micelles dissolve over a fairly narrow temperature range and the mixture forms a single homogeneous phase, in which the copolymer molecules are dispersed at random. Within the region of strong incompatibility the micelle size remains essentially independent of change in temperature. In the adjoining region of intermediate degree of compatibility the micelle core size at first decreases but subsequently passes through a minimum before

increasing again as the dissolution temperature is approached.

The finding that significant amounts of polybutadiene can be present in the micelle cores is unexpected. Under identical conditions a styrene homopolymer with molecular weight equal to that of the copolymer styrene block will barely dissolve any butadiene homopolymer.³⁶ Accordingly, it is important to enquire whether the occurrence of η values below unity might not result from errors in their evaluation. In equation (14) the second term is to account for the copolymer molecules dissolved in the homopolymer matrix surrounding the micelles. In writing this term it is assumed that the block copolymer molecules are not allowed to penetrate the coronae at all. Any error in this assumption or errors in the values of ϕ_c and ζ (the ratio of the overall radius to the core radius) would affect the value of this term as a whole. The relative magnitude of the second term in comparison to the first term increases as the temperature is raised toward the dissolution temperature and thereby ϕ_c approaches the overall polymer concentration ϕ . The error arising from this source would then be the highest with mixtures containing the smallest amount of the copolymer. However, the tendency for η to decrease almost linearly with increasing temperature is very similar for all concentrations of a given copolymer, as seen in Figure 6, and suggests that the η values smaller than unity cannot be attributed to the error in the second term of equation (14).

Another possible source of error in η arises in the calibration of the X-ray scattering instrument to determine the

conversion factor for scaling the observed intensity into absolute electron units, as mentioned already. There is no reason to believe that this conversion factor changes with change in the sample temperature when the rest of the instrument is always at room temperature. The η values smaller than anticipated mean that the scattered intensity observed is not as strong as would have been otherwise. We interpret this to mean that the electron density contrast between the core and the surrounding matrix is reduced as a result of dilution of styrenes in the core by butadiene units. We may inquire about another possibility by which the scattered intensity could be reduced. If the mixture were to undergo macroscopic phase separation, with the phase rich in copolymer precipitating out, then the reduced amount of copolymer present in the micelle-containing phase would reduce the number density of micelles in the system. No evidence for occurrence of such macrophase separation was noted in the concentration range studied in this work. Although some of the more concentrated mixtures appear slightly turbid, no change in their appearance or in the scattering intensity can be noted with time even when the sample was observed for several days. Attempts to induce separation into layers using a laboratory centrifuge have been similarly unsuccessful.

The value of η lower than unity merely indicates that the styrenes in the core are diluted by butadienes, without suggesting the source of the butadienes. Because of its low molecular weight, the homopolymer is most likely the major component to swell the core, but some of the butadiene blocks of

the copolymer may also find themselves there. The radii of core given in Figure 3 are all larger than the average end-to-end distance of the respective styrene blocks involved, suggesting that they are considerably stretched. When no diluent is present, such stretching is forced upon them by the necessity to maintain a uniform mass density. With diluent present, the entropic cost of stretching the chain could be somewhat alleviated by distributing the diluent molecules more toward the center of the core. It is conceivable that in the extreme situation the core itself may acquire a two-zone structure of the butadiene inner core surrounded by styrene shell, which in turn is surrounded by the butadiene corona, or that the micelle may even adopt a shape different from sphere. The data available in this work are not sufficient by themselves to ascertain whether any of these possibilities might have been realized. Our analysis of the X-ray intensity data is based on the assumption of spherical cores having uniform electron density in it. If this assumption turns out to be not strictly correct, then some of the numerical results, especially those at high temperatures, could be modified, but the extent of such modification would be small, and in any case all the semi-quantitative conclusions drawn should remain valid.

ACKNOWLEDGMENT

This work was supported in part by the Office of Naval Research.

REFERENCES

1. Roe, R.-J., Fishkis, M., and Chang, J. C., *Macromolecules*, 1981, 14, 1091.
2. Leibler, L., *Macromolecules*, 1980, 13, 1602.
3. Zin, W.-C. and Roe, R.-J., *Macromolecules*, 1984, 17, 183.
4. Roe, R.-J. and Zin, W.-C., *Macromolecules*, 1984, 17, 189.
5. Leibler, L. and Pincus, P. A., *Macromolecules*, 1984, 17, 2922.
6. Rigby, D. and Roe, R.-J., *Macromolecules*, 1984, 17, 1778.
7. Leibler, L., Orland, H., and Wheeler, J. C., *J. Chem. Phys.*, 1983, 79, 3550.
8. Noolandi, J. and Hong, K. M., *Macromolecules*, 1983, 16, 1443.
9. Roe, R.-J., to be published.
10. Krause, S., Lu, Z.-H., and Iskandar, M., *Macromolecules*, 1982, 15, 1076.
11. Roe, R.-J., Chang, J. C., Fishkis, M., and Curro, J. J., *J. Appl. Crystl.*, 1981, 14, 139.
12. Strobl, G. R., *Acta Cryst.*, 1970, A26, 367.
13. Debye, P., *Phys. Z.*, 1927, 28, 135.
14. Fournet, G., *Acta Cryst.*, 1951, 4, 293.
15. Guinier, A., Fournet, G., Walker, C. B., and Yudowitch, K. L., "Small-Angle Scattering of X-rays," John Wiley, New York, 1955.
16. Percus, J. K. and Yevick, G. J., *Phys. Rev.*, 1958, 110, 1.
17. Cebula, D. J., Ottewell, R. H., and Ralston, J., *J. Chem. Soc., Faraday Trans. I*, 1981, 77, 2585.
18. Kinning, D. J. and Thomas, E. L., *Macromolecules*, 1984, 17, 1712.
19. Vrij, A., *J. Chem. Phys.*, 1979, 71, 3267.
20. Van Beurten, P. and Vrij, A., *J. Chem. Phys.*, 1981, 74, 2744.
21. Blum, L. and Stell, G., *J. Chem. Phys.*, 1979, 71, 42.

22. Kotlarchyk, M. and Chen. S.-H., J. Chem. Phys., 1983, 79, 2461.
23. Aragon, S. R. and Pecora, R., J. Chem. Phys., 1976, 64, 2395.
24. Ashcroft, N. W. and Lekner, J., Phys. Rev., 1966, 145, 83.
25. Ruland, W., J. Appl. Cryst., 1971, 4, 70.
26. Roe. R.-J., J. Appl. Cryst., 1982, 15, 182.
27. Hashimoto, T., Todo, A., Itoi, H., and Kawai, H., Macromolecules, 1977, 10, 377.
28. Todo, A., Hashimoto, T., and Kawai, H., J. Appl. Cryst., 1978, 11, 558.
29. Hashimoto, T., Shibayama, M., and Kawai, H., Macromolecules, 1980, 13, 1237.
30. Hashimoto, T., Fujimura, M., and Kawai, H., Macromolecules, 1980, 13, 1660.
31. Hashimoto, H., Fujimura, M., Hashimoto, T., and Kawai, H., Macromolecules, 1981, 14, 844.
32. Berney, C. V., Cohen, R. E., and Bates, F. S., Polymer, 1982, 23, 1222.
33. Richards, R. W. and Thomason, J. L., Polymer, 1983, 24, 1089.
34. Selb, J., Marie, P., Rameau, A., Duplessix, R., and Gallot, Y., Polymer Bulletin, 1983, 10, 444.
35. Polymer Handbook, Second Edition, Section V, Brandrup, J. and Immergnt, E. H., Eds., John Wiley, 1975.
36. Roe, R.-J. and Zin, W.-C., Macromolecules, 1980, 13, 1221.
37. Richardson, M. J. and Savill, N. G., Polymer, 1977, 18, 3.

LEGEND TO FIGURES

- Figure 1. The scattered X-ray intensity $I(s)$ (after correction for slit-smearing effect) is plotted against s ($= 2 \sin (\theta/\lambda)$) to illustrate the fit achieved by the calculated curves. The points are the experimental data obtained at 30°C with a mixture containing 8% sample 50/50, the solid curve is the calculated best fit achieved by adjustment of four parameters including the polydispersity parameter Z , and the broken curve is the best fit obtained with monodispersity assumption. Note the low angle peak which arises as a result of interparticle interference.
- Figure 2. The points are the observed intensity data (after desmearing) obtained at 30°C with a mixture containing 3% sample 75/25, the solid curve is the best fit obtained with polydispersity effect included, and the broken curve is the best fit obtained with monodispersity assumption.
- Figure 3. The z-average radius $\langle R \rangle_z$ of the core is plotted against temperature for the three series of mixtures indicated.
- Figure 4. The plot illustrates the method used for determining the critical micelle concentration. The X-ray intensity $I(s)$ at $s = 0.030\text{nm}^{-1}$ obtained with mixtures containing sample 75/25 is plotted against the concentration of the copolymer. The data points

obtained at a temperature lie on a good straight line, and its extrapolation to $I(s) = 0$ gives the critical micelle concentration.

Figure 5. The critical micelle concentrations of the three copolymer samples in polybutadiene are plotted against temperature.

Figure 6. Temperature variation of the volume fraction η of styrene in micelle cores. Sample 75/25 -- solid square, 1%; solid triangle, 1%; solid diamond, 1.5%; solid circle, 3%. Sample 50/50 -- open square, 1%; open triangle, 2%; open diamond, 4%. Sample 25/75 -- solid circle, 14%.

Figure 7. Temperature variation of the number of micelles per unit volume of mixture.

Table 1
Characterization of Samples Used

	<u>Diblock Copolymer</u>			<u>Polybutadiene</u>
	<u>25/75</u>	<u>50/50</u>	<u>75/25</u>	
M_n	27000	25000	21000	2350
M_w/M_n	1.04	1.04	1.05	1.13
% trans. 1.4	42	45	48	53
% cis. 1.4	28	24	24	41
Styrene content (wt.%)	27.0	52.2	76.6	N/A

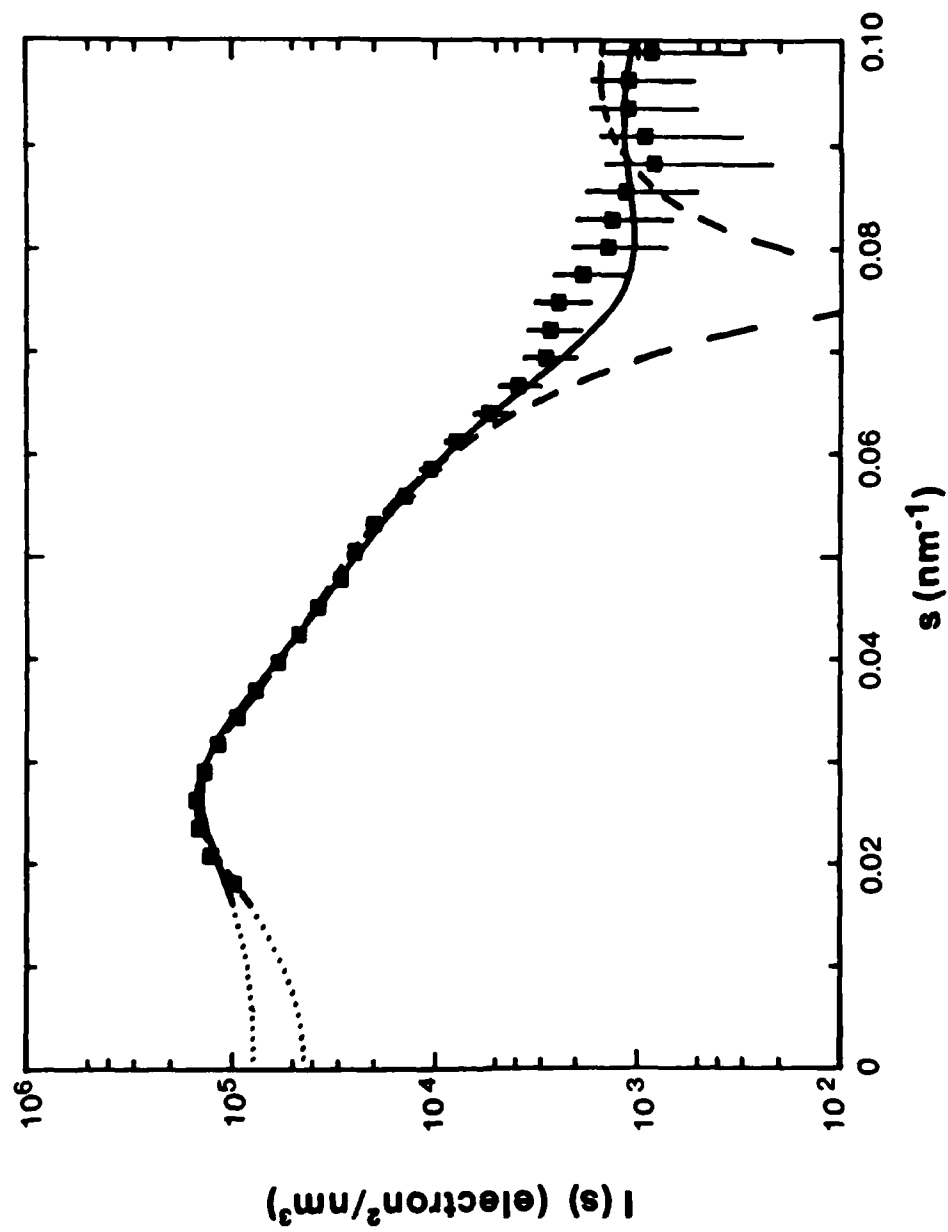


Figure 1

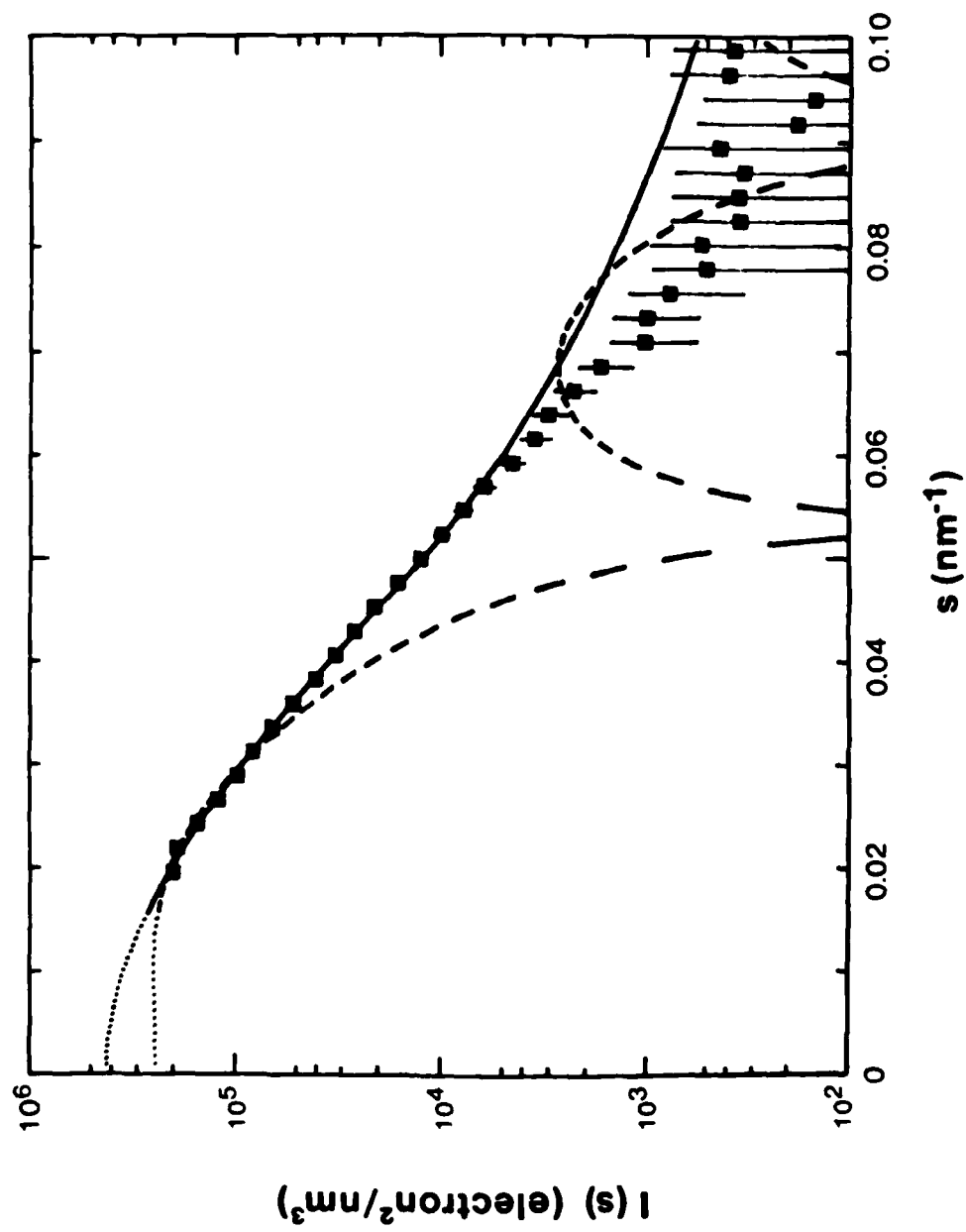


Figure 2

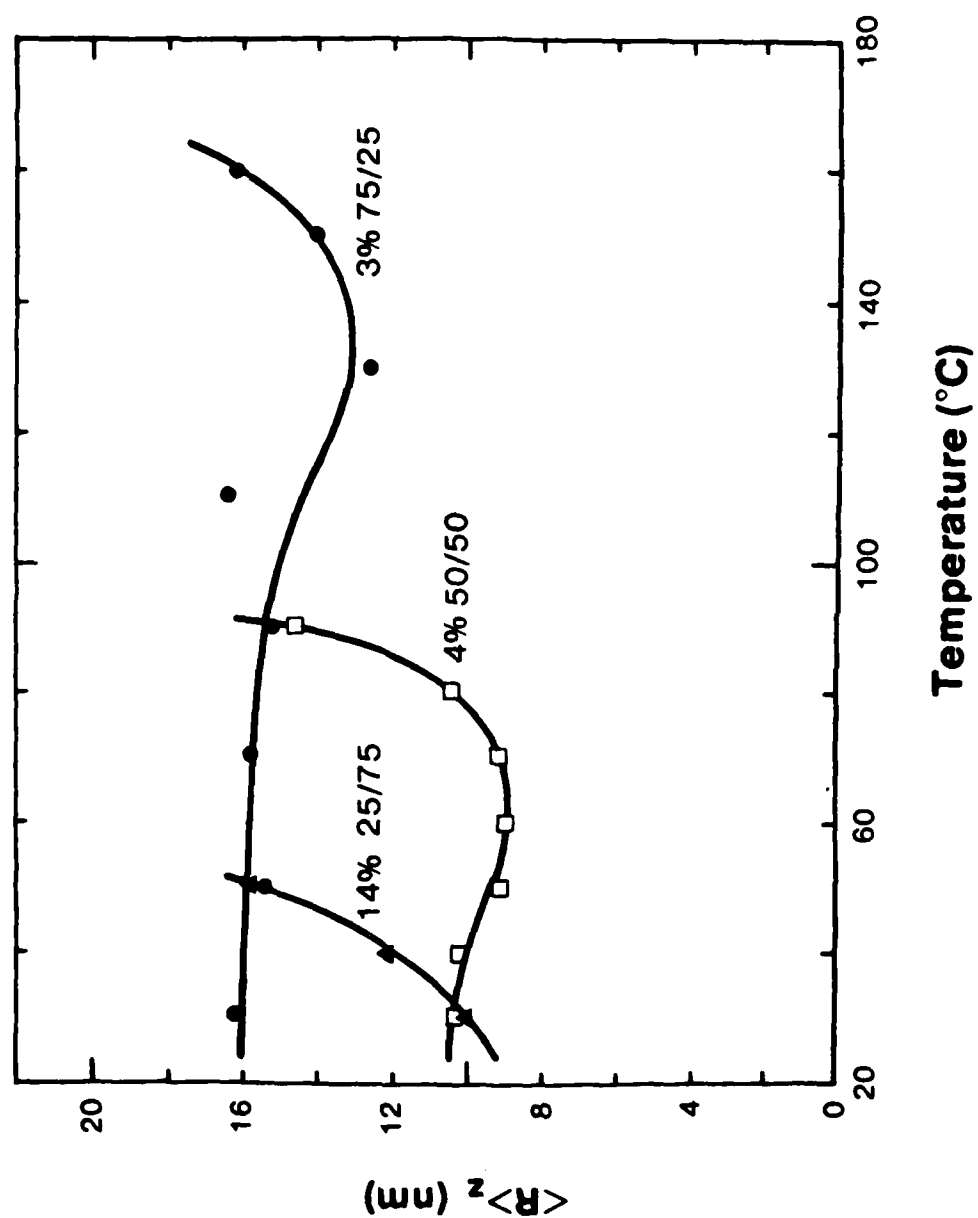


Figure 3

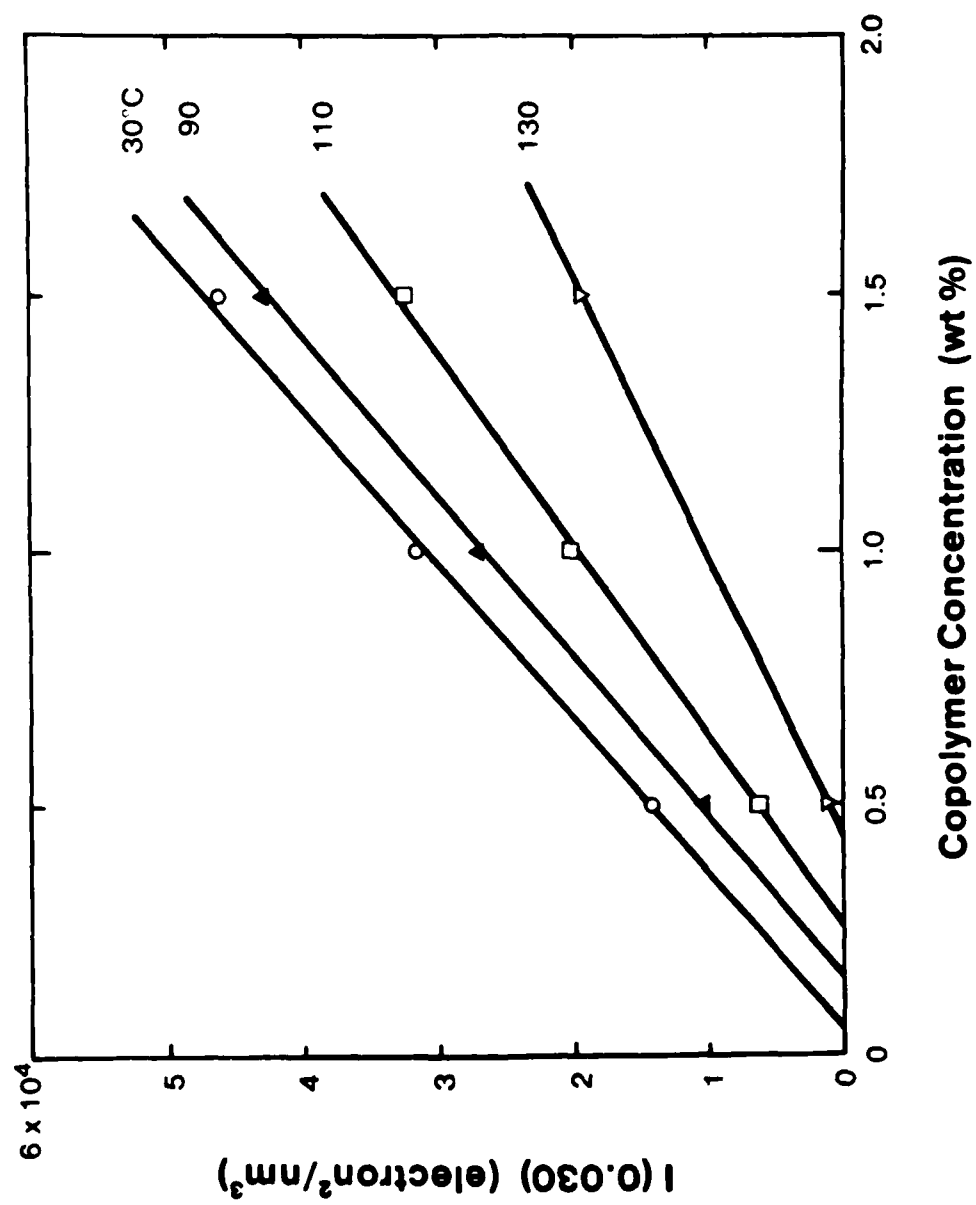


Figure 4

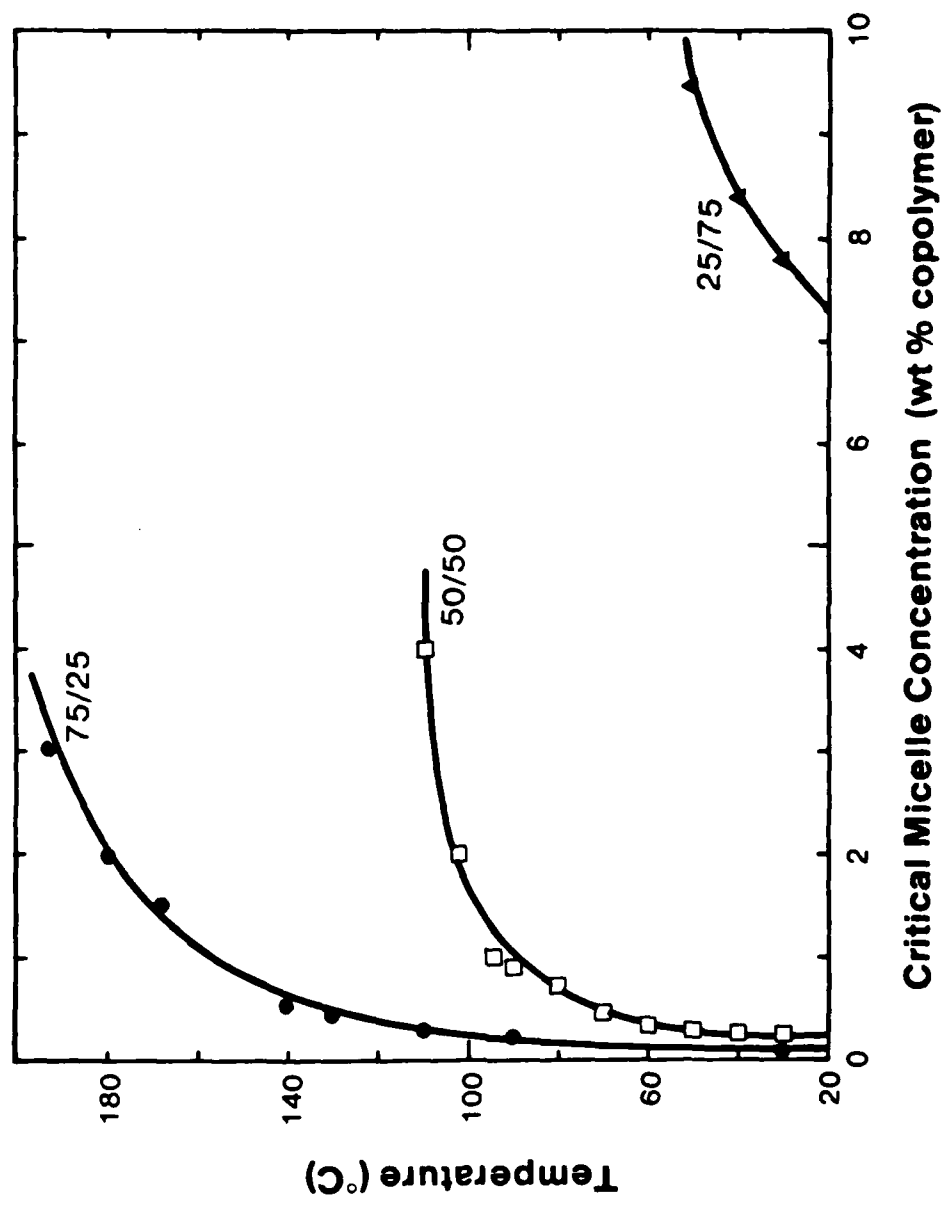


Figure 5

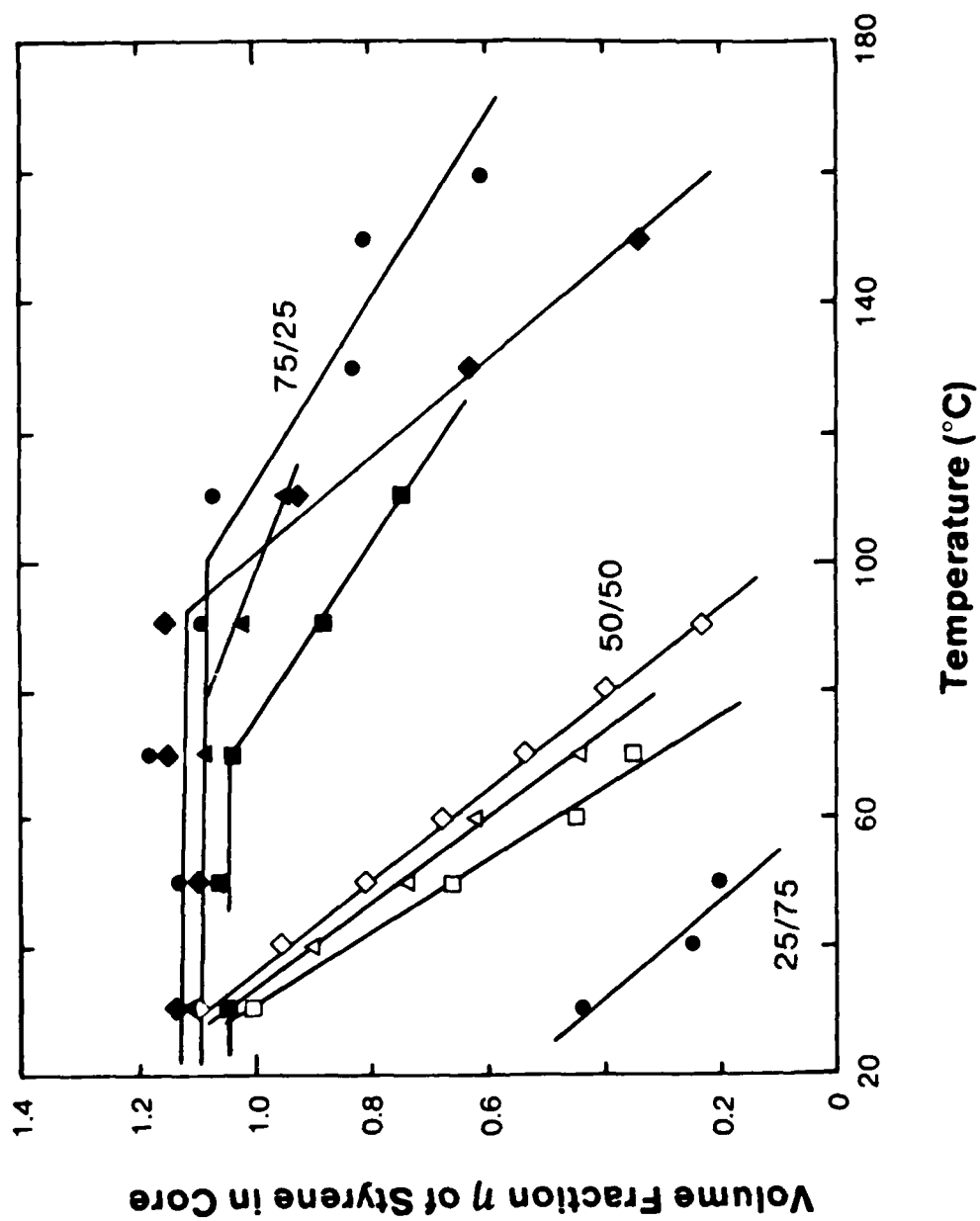


Figure 6

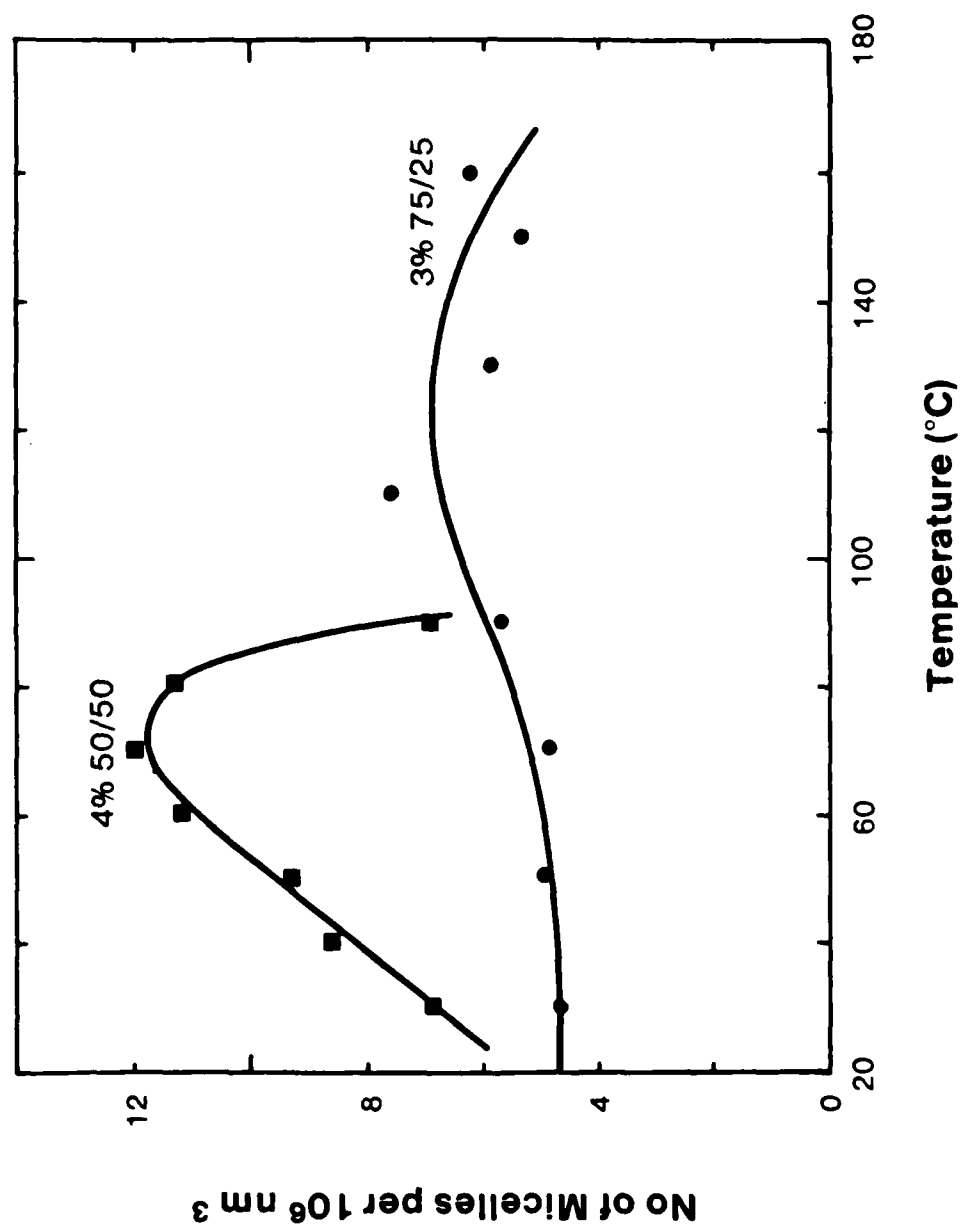


Figure 7

TECHNICAL REPORT DISTRIBUTION LIST, GEN

	<u>No. Copies</u>		<u>No. Copies</u>
Office of Naval Research Attn: Code 413 800 N. Quincy Street Arlington, Virginia 22217	2	Dr. David Young Code 334 NORDA NSTL, Mississippi 39529	1
Dr. Bernard Douda Naval Weapons Support Center Code 5042 Crane, Indiana 47522	1	Naval Weapons Center Attn: Dr. Ron Atkins Chemistry Division China Lake, California 93555	1
Commander, Naval Air Systems Command Attn: Code 310C (H. Rosenwasser) Washington, D.C. 20360	1	Scientific Advisor Commandant of the Marine Corps Code RD-1 Washington, D.C. 20380	1
Naval Civil Engineering Laboratory Attn: Dr. R. W. Drisko Port Hueneme, California 93401	1	U.S. Army Research Office Attn: CRD-AA-IP P.O. Box 12211 Research Triangle Park, NC 27709	1
Defense Technical Information Center Building 5, Cameron Station Alexandria, Virginia 22314	12	Mr. John Boyle Materials Branch Naval Ship Engineering Center Philadelphia, Pennsylvania 19112	1
DTNSRDC Attn: Dr. G. Bosmajian Applied Chemistry Division Annapolis, Maryland 21401	1	Naval Ocean Systems Center Attn: Dr. S. Yamamoto Marine Sciences Division San Diego, California 91232	1
Dr. William Tolles Superintendent Chemistry Division, Code 6100 Naval Research Laboratory Washington, D.C. 20375	1		

END

FILMED

12-85

DTIC